Camphor pathway redux: functional recombinant expression of 2,5- and 3,6-diketocamphane monooxygenases of Pseudomonas putida ATCC 17453 with their cognate flavin reductase catalyzing Baeyer-Villiger reactions

doi: 10.1128/AEM.03958-12

Appl. Environ. Microbiol., 79: 3282–3293 (2013)

Camphor Pathway Redux: Functional Recombinant Expression of 2,5- and 3,6-Diketocamphane Monooxygenases of *Pseudomonas putida* ATCC 17453 with Their Cognate Flavin Reductase Catalyzing Baeyer-Villiger Reactions

Hiroaki Iwaki,[1] Stephan Grosse,[2] Hélène Bergeron,[2] Hannes Leisch,[2] Krista Morley,[2] Yoshie Hasegawa,[1] and Peter C.K. Lau*[2,3,4]

Department of Life Science & Biotechnology and ORDIST, Kansai University, Suita, Osaka, 564-8680, Japan,[1] *National Research Council Canada, Montreal, Quebec H4P 2R2, Canada,*[2] *McGill University, Departments of Chemistry and Microbiology & Immunology, McGill University, Montreal, Quebec H3A 2B4, Canada*[3]*, and FQRNT Centre in Green Chemistry and Catalysis, Montreal, Quebec, Canada*[4]

Running title: CAMPHOR PATHWAY TYPE II BVMOs

Abstract Whereas the biochemical properties of the monooxygenase components that catalyze the oxidation of 2,5-diketocamphane and 3,6-diketocamphane (2,5-DKCMO and 3,6-DKCMO, respectively) in the initial catabolic steps of (+) and (–) isomeric forms of camphor metabolism in *Pseudomonas putida* ATCC 17453 are relatively well characterized, the actual identity of the flavin reductase (Fred) component that provides the reduced flavin to the oxygenases is hitherto ill-defined. In this study, a 37-kDa Fred was purified from camphor-induced culture of *P. putida* ATCC 17453 and this facilitated cloning and characterization of the requisite protein. The active Fred is a homodimer with a subunit molecular mass of 18-kDa that uses NADH as electron donor (K_m = 32 μM) and it catalyzes the reduction of FMN (K_m = 3.6 μM; k_{cat} = 283 s^{-1}) in preference to FAD (K_m = 19 μM; k_{cat} = 128 s^{-1}). Sequence determination of ~40-kb of the camphor (CAM) degradation plasmid revealed the locations of two isofunctional 2,5-DKCMO genes (*camE*$_{25\text{-}1}$ for 2,5-DKCMO-1, and *camE*$_{25\text{-}2}$ for 2,5-DKCMO-2) as well as that of 3,6-DKCMO-encoding gene (*camE*$_{36}$). In addition, by pulsed-field gel electrophoresis, the CAM plasmid was established to be linear and ~533-kb in length. To enable functional assessment of the two-component monooxygenase system in Baeyer-Villiger oxidations, recombinant plasmids expressing Fred in tandem with the respective 2,5-DKCMO and 3,6-DKCMO encoding genes in *Escherichia coli* were constructed. Comparative substrate profiling of the isofunctional 2,5-DCKMOs did not yield obvious differences in Baeyer-Villiger biooxidations but they are distinct from 3,6-DKCMO in the stereoselective oxygenations with various mono- and bicyclic ketone substrates.

INTRODUCTION

In the history of *Pseudomonas* genetics, camphor metabolism by *P. putida* ATCC 17453 (NCIMB 10007; referred herein as strain PpCam), mediated by the "large" incompatibility group 2 (incP2) transmissible CAM plasmid, may be regarded as the genus' oldest known profession (1-3). Pioneering work by the laboratory of the late Gunsalus and coworkers dated back half a century ago (1, 4-6) A schematic representation of the catabolic steps of conversion of the (+) and (–) isomeric forms of camphor (compounds **1** and **2**, respectively) in strain PpCam that includes contributions from this study is shown in Fig. 1. In this pathway, the genetics and biochemistry of the cytochrome P450-containing enzyme complex (CamCAB) and 5-*exo*-hydroxycamphor dehydrogenase (CamD) that led to the formation of the 2,5-diketocamphane or 3,6- diketocamphane (compounds **3** and **4**, respectively in Fig. 1) are well understood (7-12).

Metabolism of compound **3** or **4** proceeds via the action of a Baeyer-Villiger monooxygenase (BVMO) system known as 2,5-diketocamphane monooxygenase (2,5DKCMO) or 3,6-diketocamphane monooxygenase (3,6-DKCMO) (9, 13, 14). Both are prototype members of type 2 BVMOs (15) the fact that they are FMN and NADH-dependent, in sharp contrast to the more frequently found type 1 BVMOs that use FAD as a prosthetic group and NADPH as a cofactor. BVMOs in general are virtuous green reagents (using molecular oxygen as oxidant and producing only water as a byproduct) that have a proven record of assessing high chemo-, regio- and enantio-selectivity in a variety of oxidation reactions that include epoxidation and S- and N-heteroatom oxidations (16-20).

It is generally known that either 2,5-DKCMO or 3,6-DKCMO consists of a homodimeric FMN-containing oxygenation component and a second component that has been referred to as an NADH dehydrogenase or NADH oxidase (14) which may be common to both flavoproteins.

In keeping with the modern nomenclature of the FMN-dependent two-component monooxygenase systems (21), we adopt the name flavin reductase or Fred in this study.

Both the DKCMO oxygenating subunits of strain PpCam have been purified to homogeneity and shown to be discrete enzymes having different molecular weights (subunit M_r 37-40 kDa vs. 38-40.3 kDa) and isoelectric points (4.6 vs. 5.5) (9, 13, 14). Also, both DKCMOs have been crystallized, but only the structure of 3,6-DKCMO has been solved to 2.00 Å resolution (PDB id: 2wgk, 22-24). Recently, Kadow et al (25, 26) described the gene structures of a 2,5-DCKMO and 3,6-DCKMO and reported biotransformation results based on a presumed endogenous reductase from the *Escherichia coli* host that could complement the DKCMO activity. Needless to say, without a *bona fide* reductase the reported activities were extremely low if at all reliable. Indeed, the majority of the biotransformation experiments carried out in the past by pioneering lab of Willetts using the two enantiomeric systems had been conducted in whole *P. putida* cells. A mixture of the 2,5-DKCMO and 3,6-DKCMO enzymes has been referred to as MO1 to distinguish it from the MO2 activity of 2-oxo-Δ^3-4,5,5-trimethylcyclopentenylacetyl-CoA monooxygenase (OTEMO), a type 1 BVMO (15, 26-29). Importantly, each DKCMO enzyme was shown to have absolute specificity for substrates of the respective enantiomeric series of camphor-ketones and also shown to have useful enantioselective properties (27, 30-33). These enzymes are also active on the respective camphor enantiomer (13, 14, 34).

The following are brief accounts of previous attempts to isolate the reductase component of the DKCMO system. Conrad et al (4-6) described this as an "electron transport oxidase" believed to catalyze the FMN-mediated reduction of oxygen to hydrogen peroxide by NADH. However, Trudgill et al. (35, 36) demonstrated that this enzyme of 36-kDa purified from (+)-camphor grown cells of *P. putida* strain C_1B (= ATCC 17453; 13, 14, 22) did not directly

93 transfer electrons to oxygen and introduced the name NADH:(acceptor) oxidoreductase; also
94 known by its trivial name as NADH dehydrogenase. The purified enzyme was found to bind
95 FMN very weakly (K_d of 0.45 μM) in a 1:1 ratio. It was further characterized to contain two
96 flavin-binding sites and would loosely interact with the oxygenating component to form an
97 active complex. Since these studies there had been no further work on the enzyme.
98 In this study we set out to identify and clone the gene for a flavin reductase (Fred) from strain
99 PpCam that is requisite to oxygenating activity. The new Fred-encoding gene was assembled
100 with the corresponding DKCMO gene for the first time to facilitate Baeyer-Villiger oxidations in
101 a recombinant format. In addition, we applied pulsed-field gel electrophoresis to uncover new
102 salient features of the prototypical CAM plasmid. This study was also set out to sequence CAM
103 plasmid DNA beyond the well established but limited *cam* operon locus with the goal to
104 localize the positions of the 2,5- and 3,6-DKCMO encoding genes with respect to both known
105 and potential new genes that may be assigned to the complete CAM degradation pathway.
106
107 **MATERIALS AND METHODS**
108 **Bacterial strains and culture conditions.** *P. putida* ATCC 17453 (strain PpCam) and *E. coli*
109 strains were grown at 30 °C and 37 °C, respectively, and routinely cultured in Luria-Bertani
110 (LB) broth or media as previously described (29). When necessary, the media were
111 supplemented with ampicillin (Ap, 100 μg/ml). Growth of strain PpCam on (+) or (–) or racemic
112 camphor (0.3-0.5%) as sole carbon source was carried out in mineral medium as originally
113 described (13, 14).
114 **CAM plasmid size determination.** Megaplasmid detection was first performed using the in-
115 well cell lysis technique (37) as described in the supplemental material accompanying Fig. S2.

To determine the molecular sizes of the large plasmids, their profiles were determined by using nuclease S1 treatment followed by pulsed-field gel electrophoresis (PFGE) as originally described by Barton et al. (38) with some modifications. Briefly, genomic DNAs of *Sphingomonas aromaticivorans* F199 used as control (39) and PpCam were first embedded in agarose plugs. To linearize potential circular megaplasmids, 4 mm slices of agarose plugs were cut out and equilibrated in S1 buffer (50 mM NaCl, 30 mM sodium acetate, pH 4.5, 5 mM $ZnSO_4$) for 30 min, and then digested with 8 U of *Aspergillus oryzae* S1 nuclease (Fermentas EN0321) for 15 min at 37 °C. Slices of the plug incubated only in S1 buffer were run in parallel to detect non-linearized megaplasmids. The reaction was stopped by the addition of 20 µL of EDTA (0.5 M, pH 8). The plugs were loaded immediately on a 0.8% agarose gel in 1x TBE buffer and the wells were sealed by addition of agarose. The gel was run at 4 °C for 65 hours using a Q-Life Autobase PFGE system with ROM card No. 5 for resolution of 100- to 1100-kb DNA fragments (40). The gel was stained with 0.5 µg/mL ethidium bromide for 1 hour, washed in distilled water for 50 min, then photographed.

Cloning and sequencing of additional genes in the CAM pathway. Recombinant techniques were carried out according to Sambrook et al (41). Cloning and localization of the 2,5-DKCMO-1 encoding gene in a 6.8-kb BamHI fragment of PpCam total DNA in an *E. coli* recombinant plasmid pCAM200 has been described previously (29). Additional cloning of a ~26-kb DNA segment of PpCam DNA downstream of the *camDCAB* operon in four overlapping clones (13-kb BamHI fragment in pCAM300; 5.5-kb Nsi fragment in pCAM500; 8.1-kb BamHI fragment in pCAM600; and 7.1-kb BglII fragment in pCAM700), and analysis of the DNA sequence determination are described in the supplemental material SM1/TableS1/Table S2. A summary of the established and predicted gene organization is shown in Fig. 2.

Construction of overexpression clones of DKCMOs. The isopropyl-ß-D-thiogalactopyranoside (IPTG)-inducible *E. coli* pSD80 vector (42) was used to carry the respective *Pfu* DNA polymerase-amplified DKCMO-encoding genes using the forward and reverse primers with built-in EcoRI or PstI restriction sites listed in Supplemental material Table S1. The resulting clones transformed in *E. coli* BL21 cells are designated pDKCMO25-1, pDKCMO25-2, and pDKCMO36, respectively. The cloned inserts were verified by DNA sequencing as previously described (43, 44).

Purification of recombinantly produced DKCMOs. All purification procedures were performed at 4 °C on an ÄKTAexplorer™ 100 Air chromatography system (GE Healthcare). Crude enzyme extract of the respective stock culture was processed essentially as previously described for OTEMO (29). A three-step purification scheme that led to electrophoretic purity of the proteins was developed as described in the supplemental material that accompanies Fig S4.

CD spectroscopy and determination of melting point (T_m). CD spectra of the DKCMOs were recorded on a Jasco J-815 spectrometer operating with the Spectra Manager software. Temperature was controlled by a Jasco PFD-452S peltier unit. Purified protein solutions were desalted using a HiPrep Desalting column (26/10) previously equilibrated with 20 mM Na-Phosphate buffer (pH 7.0). Final protein concentration was adjusted to about 0.1 mg/ml and the respective CD spectrum was recorded between 200 and 260 nm using a Quartz cuvette (ID = 0.1 cm). Blanks containing buffer only were prepared and used as baseline. Temperature dependent protein unfolding was monitored at 222 nm with thermal profiles ranging from 20 to 80 °C (2°C min^{-1}). Thermodynamic parameters (T_m, ΔH, ΔS, ΔG) were calculated using the Spectra Manager software.

DKCMO cell free assays. Enzyme activity was routinely detected in a reaction mixture (0.5 mL) containing Tris/HCl buffer (50 mM, pH 7.5), 3.3 mM NADH, 0.03 mM FMN, 30 mU of formate dehydrogenase (FDH), 50 mM sodium formate, 10-50 mU Fred and about 0.4 mg of the respective DKCMO. The reaction was started by adding (+)-camphor (2 mM) for the 2,5-DKCMOs and (−)-camphor for 3,6-DKCMO, respectively. Controls contained all components, but DKCMO or Fred. Samples were incubated for 10, 20, 30, 60, 90 min, respectively, and reaction was stopped by adding 0.5 ml of acetonitrile. Precipitated protein was removed by centrifugation and substrate depletion was followed by HPLC using a C_{18} column. An isocratic method was used with $H_2O/CH_3CN/CH_3COOH$ (598/400/2) as mobile phase (0.5 ml/min) and UV-detection at 220 nm on a Waters Millennium system.

Detection and purification of an FMN-reductase (Fred) from strain PpCam. Fred activity was assayed in a reaction mixture (1 ml) containing Tris/HCl buffer (50 mM, pH 7.5), 0.07 mM NADH, and 0.025 mM FMN, and the reaction initiated by the addition of an appropriate amount of enzyme. The decrease in absorbance at 340 nm due to the oxidation of NADH was monitored. Blanks containing all components except the substrate (FMN) were prepared. Specific activity was defined as the amount of protein that oxidizes one µmole of NADH ($\varepsilon = 6.22$ L mmol^{-1} cm^{-1}) per minute (U) per milligram of protein (U/mg).

Purification of Fred was performed at 4 °C on an ÄKTAexplorer™ 100 Air chromatography system (GE Healthcare). The crude extract of (+)-camphor grown culture of PpCam obtained by cell breakage via French press was loaded on a DEAE-Sepharose FF column (XK50/20) equilibrated with 20 mM sodium phosphate buffer (pH 7.0). The flow rate was 4 ml/min. The column was washed with the same buffer until no protein could be detected in the flow through, and enzyme was subsequently eluted with a linear gradient of 0 – 0.2 M NaCl. Active fractions

were pooled and concentrated by ultrafiltration (200 mL stirring cell, Amicon, USA, using a YM3 membrane) and applied to a Ni-NTA column (16/10) previously equilibrated with 20 mM sodium phosphate buffer containing 0.15 M NaCl. The flow through containing the active protein was collected, concentrated and applied to a HiLoad Superdex 200 prep grade column (16/60) which was previously equilibrated with 20 mM sodium phosphate buffer (pH 7.0) containing 0.15 M NaCl. Protein was eluted with the same buffer (flow rate of 1.5 mL/min) and collected in 2 ml fractions.

Kinetic parameters. Kinetic parameters of the Fred were determined by using the double-reciprocal transformation (Lineweaver-Burk plot) of the Michaelis-Menten equation under steady-state conditions. Results were verified by Eisenthal-Cornish-Bowden direct plots. Initial reaction rates were measured at 25 °C in Tris/HCl buffer (50 mM, pH 7.5) by using total substrate and coenzyme concentration between 1-100 μM, respectively.

N-terminal and internal peptide sequencing and chemical digestion of Fred. Purified Fred, separated by SDS-PAGE was blotted to a polyvinylidene difluoride (PVDF) membrane (Bio-Rad, USA). N-terminal sequence determination was performed with a sequencer (473A; Applied Biosystems) by the Edman method (45). Phenylthiohydantoin amino acids were analyzed by HPLC with a reversed-phase column. For internal peptide sequencing, purified Fred was adjusted to 1 mg/ml and chemically digested using the following chemicals: o-iodobenzoic acid (46), cyanogen bromide (47), and formic acid (48). Cleaved protein fragments were separated by SDS-PAGE (15% PA), and peptide sequences of the cleaved protein fragments were determined as described above.

Cloning of the flavin reductase-encoding gene (*fred*) from strain PpCam. Two primers with the following sequences were designed based on the determined peptide sequences,

207 ATDPQWF and PPLVAF, respectively: fRED07-5'spec and 2SG-REV1 (Table S1). Following
208 the addition of a 3'-overhang, the amplified 150-bp product was cloned in the TOPO TA cloning
209 vector pCR2.1-TOPO (Invitrogen cat.:#K4500-01) and transformed in *E. coli* Top 10, and the
210 resulting plasmid was designated pCR2.1TOPO-frgPCR G1#3 and sequenced to confirm its
211 identity. To clone the complete *fred* gene, the GenomeWalker Universal Kit (Clontech #cat:
212 638904**)** was utilized and genomic libraries from strain PpCam were generated by digestion with
213 different blunt end cutting endonucleases (EcoRV, PvuII and StuI) and by adapter ligation at the
214 ends of the resulting DNA fragments. These libraries were utilized as independent templates in
215 three different PCR reactions. One gene specific primer, GSP1RED (Table S1) from the
216 pCR2.1TOPO-frgPCR G1#3 sequence was used in combination with a kit adapter primer (AP1)
217 in a first PCR reaction. Subsequently, 1 µL of the first PCR (diluted 50-fold) served as a
218 template in a secondary PCR, applying one nested gene-specific primer, GSP2RED (Table S1)
219 along with a nested kit adapter primer (AP2). The resulting products were cloned into pCR2.1-
220 TOPO and the sequences of the inserts were determined.

221 The DNA fragment carrying *fred* was amplified by using Platinum *Pfx* DNA polymerase
222 (Invitrogen) with two PCR primers with NdeI and EcoRI restriction sites (fred07Nde-f and
223 fred07Eco-r in Table S1) to facilitate subsequent cloning. The amplified DNA fragment was
224 purified from agarose gel, digested with the restriction enzymes and cloned in the pET17b
225 vector. *E. coli* BL21(DE3)/pLysS containing the plasmid pET-Fred07#3 was cultivated in 250
226 mL of LB medium containing 100 µg/mL of ampicillin at 30 °C. When the culture reached an
227 OD_{600} of 0.6, IPTG was added to a final concentration of 1 mM in the medium. The cells were
228 further cultured overnight, then harvested by centrifugation.

Construction of tandem clones: CamE$_{25\text{-}1}$+Fred, CamE$_{25\text{-}2}$+Fred and CamE$_{36}$+Fred in pSD80. All tandem clones were constructed using the MultiSite Gateway® Pro Kit (Invitrogen). For each DKCMO (CamE) clone, the *tac* promoter and the specific *camE* gene were amplified with Platinum Pfx DNA polymerase (Invitrogen) as follows: the forward primer attB1MO (Table S1) and the reverse primers: attB5rMO1, attB5rMO2, and attB5rMO3 (Table S1) for *camE$_{25\text{-}1}$*, *camE$_{25\text{-}2}$*, and *camE$_{36}$*, respectively. The templates used for the amplification are clones pDCKMO25-1, pDKCMO25-2, and pDCKMO36. The T7 promoter and *fred* gene were amplified with Platinum Pfx DNA polymerase (Invitrogen) and the primers: attB5fred, and attB2fred (Table S1). The template for amplification was clone pET17b-Fred as described in the previous section.

The various *camE* PCR products were recombined with the pDONR 221 P1-P5r Gateway vector (Invitrogen) in separate reactions to form entry clones pDONR(2,5DKCMO-1), pDONR(2,5DKCMO-2), and pDONR(3,6-DKCMO), respectively. The *fred* PCR product was recombined with the pDONR 221 P5-P2 vector to form entry clone pDONR(Fred07). pDONR(2,5-DKCMO-1) and pDONR(Fred07) were recombined with the pSD80 destination vector, which was constructed using the Gateway Vector Conversion System (Invitrogen) via ligation of the RfA cassette (provided in the kit) with vector pSD80, which had been linearized with the restriction enzyme BamHI and blunt-ended with T4 DNA polymerase. The recombination product of the three plasmids was transformed into One Shot® Mach1™ T1^{R} chemically competent *E. coli*. The plasmid containing the double clone (pSD80-CamE$_{25\text{-}1}$-Fred) was then transformed into *E. coli* BL21(DE3) for protein expression. Identical procedures were carried out for the recombination of pDONR(2,5-DKCMO-2) and pDONR(3,6DKCMO) with

pDONR(Fred07) and the pSD80 destination vector to afford plasmids pSD80-CamE$_{25\text{-}2}$-Fred and pSD80-CamE$_{36}$-Fred, respectively.

Monooxygenase-catalyzed BV oxidations. *E. coli* BL21 harboring the respective monooxygenase (2,5-DKCMO-1, 2,5-DKCMO-2, and 3,6-DKCMO) and Fred containing plasmid was maintained on LB medium containing glycerol (50%, vol/vol) at – 80 °C. For biotransformation experiments, a fresh LB agar plate (1.5% agar) containing ampicillin (100 μg/ml) was prepared from the stock culture, and one colony was transferred to a preculture (20 ml) containing LB medium supplemented with ampicillin (100 μg/ml) and grown at 30 ºC at 200 rpm on an orbital shaker overnight. An aliquot of the suspension (2 ml) was used to inoculate LB medium (200 ml) supplemented with ampicillin (100 μg/ml) and the resulting suspension was grown at 30 ºC at 200 rpm on an orbital shaker. At an OD_{600} of 0.5 (~ 3 h) protein expression was induced by the addition of IPTG (final concentration 1 mM). The cells were allowed to grow for an additional 3 hours (OD_{600} of 2.0 - 2.2), and the cell suspension was divided into 10 ml batches. To each batch a solution of substrate in isopropanol (1 M, 30 μl) was added and the reaction flask was shaken at 30 ºC at 200 rpm on an orbital shaker. After 18 hours the cell suspension was centrifuged and the supernatant was extracted with ethyl acetate (10 ml). The layers were separated and the organic layer was dried over anhydrous sodium sulphate and filtered. The obtained solution was used for GC analysis. For retention times of starting materials and products, and details on the GC analysis, readers are referred to Supplemental material SM2.

Accession numbers. The nucleotide sequences determined in this study have been deposited in the Genbank database under accession numbers AB771747 and KC349947.

RESULTS

Linear nature of CAM plasmid. The CAM plasmid extracted by in-well cell lysis was first analyzed by traditional agarose gel electrophoresis and seen to migrate as a discrete band as well as those of the two circular plasmids of *S. aromaticivorans* strain F199 strain (pNL1 and pNL2) that were used as control (Fig. S2 in supplemental material). Next, S1 nuclease was used to linearize circular plasmids and analyzed on PFGE. As a result, two bands corresponding to the linearized pNL1 and pNL2 plasmids, calibrated by linear markers as between 145.5-194-kb, and 485-kb, respectively, are visible for the F199 strain treated with S1 nuclease (Fig. 3, lane 3). No such resolution was observed for the S1 nuclease untreated sample as expected of large circular plasmids (lane 2). On the other hand, both the S1-treated (lane 5) and non-treated (lane 4) samples of CAM plasmid afforded one band estimated at 533 kb, indicating that the CAM plasmid is linear. Further, the migration of CAM plasmid exhibited constant mobility relative to the particular size marker under other pulse conditions (not shown).

Sequenced locus, gene context and characteristics of 2,5-DKCMOs and 3,6-DKCMO. In total, a 40,450-bp region of the pCAM plasmid is now available as a result of cloning and sequencing various DNA fragments encompassing the established *camRDCAB* locus (Fig. 2). Except for the 2,5-DKCMO and 3,6-DKCMO-encoding genes described below, characteristics of the other predicted open reading frames (ORFs) which may account for additional biochemical steps of the CAM pathway are given in Table S2 and Fig. S1 of the supplemental material.

As previously reported, a 2,5-DKCMO-encoding gene (now referred to as $camE_{25\text{-}1}$ for 2,5-DKCMO-1) was localized 88-bp downstream of the OTEMO-encoding gene (*camG*) and likely co-transcribed (29). Herein we report the presence of a second copy of 2,5-DKCMO ($camE_{25\text{-}2}$;

296 for 2,5-DKCMO-2) that is localized some 23-kb downstream and encoded on an opposite strand,
297 implying divergent transcription (Fig. 2). In the same DNA strand, and separated by two
298 potential ORFs downstream, the 3,6-DKCMO encoding gene (*camE*$_{36}$) was identified. The 378-
299 amino acid protein sequence of 3,6-DKCMO was previously deposited in the RCSB protein data
300 bank as code 2WGK (www.pdb.org) that described the dimeric structure of the protein (24).
301 Identification of the N-terminal portion of this protein was aided by the available 29-amino acid
302 peptide sequence (15, 31) with one mismatch (arginine to alanine change at position 20
303 numbered from the first methionine). It is noteworthy that the subunit structure of 3,6-DCKMO
304 was superimposable with the α-subunit of luciferase with an root-mean-square deviation
305 (RMSD) of 1.83 Å (253 matching C^{α} atoms out of 378) (24).
306 The nucleotide sequences of *camE*$_{25\text{-}1}$ and *camE*$_{25\text{-}2}$ are 90% identical, the base changes result
307 in 28 amino acid substitutions along the 363-amino acid polypeptide, of which 18 are
308 conservative changes (Fig. S3a in supplemental material). Interestingly, the predicted N-terminal
309 20 amino acid sequence of 2,5-DKCMO-2 instead of 2,5-DKCMO-1 matches more closely to
310 the peptide sequence obtained by N-terminal sequencing of what was then known as 2,5-
311 DKCMO, a single protein (15, 31). The QA dipeptide at positions 2 and 3 are key determinants
312 (Fig S3b in supplemental material).
313 Approximately half of the 2,5-DKCMO and 3,6-DCKMO polypeptide sequences are
314 conserved (43.3-44.4% identity and 59.6-60.6% overall similarity), notably the presence of two
315 conserved stretches of 10 and 14 amino acids and a major deletion of 12 amino acids near the N-
316 termini of both 2,5-DKCMOs (Fig. S3a in supplemental material). A comparison of the predicted
317 secondary structures between the 2,5-DKCMO isozymes and 3,6-DKCMO shows that sequence

318 divergence appears to be localized in the extreme N-terminal region and around the
319 deletion/insertion region.

320 During the process of isolation from the respective overproducing clones, all three proteins
321 exhibited the characteristic intense yellow color of flavoproteins; however, the prosthetic group
322 (FMN) appeared to be loosely bound to the proteins. When loaded on a hydrophobic column
323 (Butyl-S-Sepharose) to which the proteins bind, FMN was eluted as a clear yellow band upon
324 washing. The now colorless enzymes, however, remained fully active in the *in vitro* assay where
325 exogenous FMN was added. Some 25 mg/L of purified 2,5-DKCMO-2, 50 mg/L of each of 2,5-
326 DKCMO-1 and 3,6-DKCMO could be obtained from the respective overproducing clones. On
327 SDS-PAGE, the purified 2,5-DKCMOs showed a M_r of 41- kDa for either isozyme (theoretical
328 40,702 and 40,574, respectively) and 44-kDa for the 3,6-DKCMO (theoretical, 42,311) (Fig. S4
329 in supplemental material). That 2,5-DKCMO is not larger than 3,6-DKCMO agrees with the M_r
330 estimated from the respective His-tagged proteins (25). Native M_r analyzed on HiLoad Superdex
331 200pg were estimated as 60-kDa, 64-kDa and 85-kDA, respectively (Fig. S5 in supplemental
332 material) supporting the dimeric nature of the proteins as previously reported (13, 14, 22, 23).

333 All 3 DKCMOs exhibit the typical CD spectrum of proteins with α-helices as the predominant
334 form of secondary structure (Fig. S6a in supplemental material). They all show minima at 222nm
335 and 208nm with a near identical profile for the two 2,5-DKCMOs but somewhat different for the
336 3,6-DKCMO especially at 208nm wavelength. Monitoring the CD at a fixed wavelength of
337 222nm while varying temperature allowed for the visualization of the protein unfolding process.
338 Interestingly, the resulting estimated melting temperatures (T_m) of the proteins (the temperature
339 where folded and unfolded protein are in equilibrium) differed substantially. These are 56±1 °C,
340 63±1 °C, and 47±1 °C, for 2,5-DKCMO-1, 2,5-DKCMO-2 and 3,6-DKCMO, respectively (Fig

S6b). By virtue of a 7°C higher T_m than that of 2,5-DKCMO-1 in the thermal denaturation experiments it can be anticipated that 2,5-DKCMO-2 has a longer shelf life time than the other counterpart.

Identification, purification and properties of Fred. In crude extracts of strain PpCam grown on (+)-camphor, FMN reductase activity (see Materials and methods for details) was detected which seemed to originate from only one enzyme that we designated Fred. This activity was not detected when the strain was grown with glucose as sole carbon source. This enzyme was subsequently purified to homogeneity using a 3-step procedure with a yield of 18% (Fig. 4). The specific activity (628.4 U/mg) of the purified Fred represents a ~260-fold purification. In the purification process a major contaminating protein was experienced during the DEAE-Sepharose chromatography where medium components and about 90% of unspecific proteins were removed. This protein that co-eluted with Fred was subsequently identified by N-terminal sequencing as camphor-5 monooxygenase ($P450_{cam}$) which is known to be induced upon growth of strain PpCam on (+)-camphor. However, in the following Ni-NTA resin chromatography, this major contaminant remained bound to the resin whereas the reductase flowed through which was collected and concentrated. The resulting homogenous protein fraction containing Fred was a clear solution showing a single absorbance maximum at 280 nm indicating it a non-flavoprotein.

The active Fred is a homodimeric protein with an apparent M_r of 37.2 kDa by size exclusion chromatography on Superdex 200 (Fig. S7 of supplemental material) and a subunit M_r of ~18 kDa by SDS-PAGE (15% PA) analysis (Fig. 4). The pH optimum was 7.5 determined in Tris/HCl buffer (50 mM). However, both activity and pH optimum appeared to depend on the buffer used, e.g., at pH 7.5 in phosphate buffer the enzyme activity was reduced to 40%; in piperazine-HCl (pH 5-6.5) and phosphate buffer (pH 6.5-7.5) both at 50 mM, Fred was found to

have an optimum activity at a lower pH of 5-6 (not shown). Optimum temperature for Fred activity was seen at between 30 and 35 °C.

Activation energy and thermostability. An activation energy of 7 kcal mol $^{-1}$ was estimated for the Fred reaction (Fig. S8 in supplemental material). Based on this data, a 10 °C increase of the reaction temperature (ΔT_{10}) would result in about 1.5 times higher rate constant. At 25 °C the free energy of activation ($\Delta G^{\ddagger}$) was calculated to be 11.7 kcal mol^{-1}.

Fred was rather stable when stored at 4 °C over several days. However, at room temperature (25 °C) the enzyme irreversibly unfolds with a half life of about 80 min (Fig. S9ab in supplemental material). At higher temperature (between 30 and 35 °C) the half life of the enzyme is even shorter, ~5-20 min.

Substrate specificity and kinetic properties of Fred. FMN and FAD are both substrates for the reductase. However, the enzyme favors FMN demonstrated by a 2-fold higher rate constant and about 5 times higher affinity (K_m = 3.6 μM, k_{cat} = 283 s^{-1}, k_{cat}/K_m = 7.9x10^7) when compared to FAD (K_m= 19 μM, k_{cat} = 128 s^{-1}, k_{cat}/K_m = 6.7x10^6). With regard to electron donor, only NADH is effective where NADPH in similar concentration acts as a very poor co-substrate. The K_m for NADH was estimated to be 32 μM. NAD^+ is a competitive enzyme inhibitor with a determined K_i of 40 mM.

Cloning of Fred-encoding gene, its sequence characteristics and gene context. Chemical cleavage of purified Fred using cyanogen bromide or formic acid yielded six peptide fragments (not shown), five of which were used to determine internal peptide sequences as well as N-terminal sequencing of the intact protein. The iodobenzoic acid treated sample did not produce any usable fragment. Degenerate primers were designed from the sequenced peptides to first clone a part of the reductase gene and eventually the entire gene as described in Materials and

387 methods. In a sequenced 4.9-kb region, Fred is flanked by a potential GTP cyclohydrolase and
388 luciferase upstream, and three potential genes downstream, all being encoded on the same DNA
389 strand (Fig. S10 in Supplemental information). Fred was cloned using the pET17b vector
390 designated pET-Fred07#3 and overexpressed in *E. coli* BL 21(DE3)/pLysS.

391 Fred consists of 170 amino acids with a predicted M_r of 18,466 Da in good agreement with
392 the experimentally determined result (Fig. 4). Three peptide sequences corresponding to amino
393 acid positions 2-21, 8-29 and 45-68 helped to establish the identity of the protein (Fig. 5). A
394 characteristic flavin reductase motif GDH (49) is found at positions 136-138. A conserved YGG
395 motif (50) is found 5-7 residues away from the C-terminus. In the BLAST search, the closest
396 homolog (59% identity) is that of a "flavin reductase-like FMN binding protein" present in the
397 genome sequence of *N. aromaticivorans* DSM 12444 (Genbank: ABD25905.1). The closest
398 homolog whose structure has been determined is nitrilotriacetate monooxygenase component B
399 (189 amino acids; NTA-MoB) derived from *Mycobacterium thermoresistibile* that was
400 characterized as a homodimer with a split-barrel motif typical of short-chain flavin reductases
401 (PDB ID 3NFW; 51).

402 It is interesting that in a phylogenetic analysis, the PpCam Fred does not cluster with
403 predicted flavin reductase counterparts originating from various *Pseudomonas* spp., e.g., *P.*
404 *putida* F1 or strain KT2440, but rather cluster with those members of the α-proteobacteria
405 particularly the *Novosphingobium* and *Sphingomonas* genera (Fig. S11 in supplemental
406 information).

407 The PpCam Fred-encoding gene is not part of the 40-kb sequenced *cam* locus or elsewhere
408 by PCR-amplication of the isolated CAM plasmid DNA (not shown). The same 4-kb gene locus
409 is not found in any of the presently sequenced *P. putida* genomes so far (not shown).

410 **Co-expression of DKCMO and Fred and enzyme activities.** Evidence for protein co-
411 production of DKCMO tandemly expressed with Fred is shown in Fig. S12 of supplemental
412 material. Of the three enzyme pairs, 2,5-DKCMO-1 and Fred gave the clearest expression as
413 seen on the SDS-PAGE. For unknown reason, the expression level of 3,6-DKCMO appeared to
414 be the weakest. Nonetheless, the biotransformation experiments (described in a later section)
415 using whole cells support the co-expression of the two proteins. In contrast, whole cells
416 expressing these oxygenating components alone showed very little activity with (+)- or (–)-
417 camphor as substrate.

418 In cell-free assays that involved an NADH-regenerating system using formate dehydrogenase
419 (FDH) and sodium formate, addition of different amounts of Fred was seen to potentiate the
420 monooxygenase activity. As an example, a ~20-fold increase in 2,5-DKCMO-2 activity due to
421 the addition of Fred is shown in Fig. 6. In two other experiments, linear dependency on the
422 concentration of Fred in the oxidation of (+)- or (–)-camphor was shown (Fig. S13 in
423 supplemental material). These experiments also showed the high specificity of the respective
424 DKCMOs toward the camphor enantiomers. Moreover, a ratio of 4:1 (DKCMO:Fred) was found
425 to be optimal for measuring enzyme activity. The pH optimum for 2,5-DKCMO-1, 2,5-
426 DKCMO-2, and 3,6-DKCMO was estimated to be 7.5, 8.0 (Tris-HCl-buffer) and 7.0 (sodium
427 phosphate buffer), respectively (not shown). Under these conditions the activities of the purified
428 2,5-DKCMO-1 and 2,5-DKCMO-2 *in vitro* were determined to be nearly identical at 1.0 U/mg
429 and 1.1 U/mg for (+)-camphor. For 3,6-DKCMO this was 0.81 U/mg with (–)-camphor.

430 **Coupled DKCMO-Fred oxidations of selected ketones.** To establish the substrate
431 acceptance and enantioselectivity of the three DKCMOs, whole-cell oxidations were carried out
432 for 18 hours in shake flasks using 3 mM of various ketones. Reaction conversions and

enantiopurities of starting materials and products were determined by chiral-phase GC as described in Materials and Methods.

(i) Terpenones. For (+)-camphor (**1**), 2,5-DKCMO-1-Fred and 2,5-DKCMO-2-Fred showed full conversion under the reaction conditions and did not convert (–)-camphor (**2**) (Table 1). Conversely, 3,6-DKCMO-Fred fully converted (-)-camphor to lactone (**2a**) and showed no conversion of (+)-camphor (**1**). Similarly, 2,5-DKCMO and 3,6-DKCMO purified from camphor-grown PpCam (13) were reported to be specific for (+)- and (–)-camphor, respectively. All three double clones were unable to convert (+)-fenchone (**6**), (–)-fenchone (**7**), and (+)-nopinone (**8**).

(ii) 2-Substituted monocyclic ketones. For the kinetic resolution of 2-substituted cyclohexanones (**9** – **12**), 2,5-DKCMO-1-Fred afforded the highest conversions and enantioselectivies among the three double clones (Table 2). 2,5-DKCMO-1-Fred oxidized the (*R*)-enantiomer of 2-phenylcyclohexanone (**12**) with an E >200. 2,5-DKCMO-2-Fred was also highly selective for the (*R*)-enantiomer (E >200), although the reaction proceeded to only 4% conversion compared to 23% for 2,5-DKCMO-1-Fred. On the contrary, 3,6-DKCMO-Fred oxidized both enantiomers of 2-phenylcyclohexanone (**12**) at the same rate (E = 1) and to only 2% conversion.

For the oxidation of alkyl-substituted cyclohexanones (**9** – **11**), all three clones were (*S*)-selective, although 3,6-DKCMO-Fred only recognized 2-methylcyclohexanone (**9**) (E = 3.2) as a substrate. 2,5-DKCMO-1-Fred and 2,5-DKCMO-2-Fred resolved 2-ethylcyclohexanone (**10**) with good enantioselectivity (E = 43 and 22, respectively) and oxidized 2-propylcyclohexanone (**11**) with moderate enantioselectivity (E = 19 and 8.5, respectively).

For the kinetic resolution of 2-alkylcyclopentanones (**13**, **14**), 2,5-DKCMO-1-Fred resolved 2-n-hexylcyclopentanone (**14**) with moderate enantioselectivity (E = 19) in favor of the (*S*)-enantiomer. 2,5-DKCMO-2-Fred oxidized 2-n-hexylcyclopentanone (**14**) with low enantioselectivity (E = 5), whereas no conversion was observed with 3,6-DKCMO-Fred. All three clones were unable to convert 2-methylcyclopentanone (**13**).

(iii) 4-Substituted cyclohexanones. Biotransformations of 4-substituted cyclohexanones (**15** - **18**) by 2,5-DKCMO-1-Fred, provided lactones with low to moderate ee values (Table 3). Oxidation of 4-methylcyclohexanone (**15**) and 4-*n*-pentylcyclohexanone (**17**) resulted in 27% and 26% ee of the respective (*R*)-lactones. Desymmetrization of 4-ethylcyclohexanone (**16**) afforded the (*R*)-enantiomer in 71% *ee*, whereas the opposite enantiomer was obtained in 61% ee for the oxidation of *tert*-butylcyclohexanone (**18**). 2,5-DKCMO-2-Fred also afforded the (*R*)-lactone of 4-ethylcyclohexanone (**16**), although in significantly higher ee (89%). In contrast, the (*S*)-lactone was obtained in 87% ee with 3,6-DKCMO-Fred. 2,5-DKCMO-2-Fred also oxidized 4-methylcyclohexanone (**15**) to the (*R*)-lactone (55% ee) but showed only traces of activity with the remaining ketones. Similarly, 4-methyl, *n*-pentyl, and *tert*-butylcylohexanone were not substrates for 3,6-DKCMO-Fred.

(iv) Bicyclic ketones. The bioconversion of [3.2.0]hept-2-en-6-one (**19**) with 2,5-DKCMO-1-Fred yielded the "normal" as well as the "abnormal" lactone in 1.3:1 ratio at 100% conversion (Table 4). The "abnormal" lactone was obtained in excellent ee (99%), whereas the ee of the "normal" lactone was signficantly lower (77%). For 2,5-DKCMO-2-Fred, the "abnormal" lactone was obtained in excellent ee (97%), and the ee of the "normal" lactone was also very high (87%). Purified 2,5-DKCMO from the native strain, which we assume is composed of both 2,5-DKCMO-1 and 2, was reported to give the "normal" and "abnormal" lactones in a 1.3:1

ratio, with product ee values of 82% and 100%, respectively (28). 3,6-DKCMO-Fred gave a 1:1.5 ratio of "normal" and "abnormal" lactones at 53% conversion. The "abnormal" lactone was obtained in 93% ee and the "normal" lactone was obtained in 57% ee. Purified 3,6-DKCMO from the native strain (28) was reported to give a 1.3:1 ratio of "normal" and "abnormal" lactones at 30% reaction conversion. The ee values of the "normal" (10% ee) and "abnormal" (72% ee) lactones were significantly lower than obtained for the biotransformation with 3,6-DKCMO-Fred.

For the oxidation of norcamphor (**20**) by 2,5-DKCMO-1-Fred, the "normal" lactone was formed in a 2.4:1 ratio with the "abnormal" lactone at ~60% reaction conversion. Product ee values were 40% ee and 57% ee, respectively. Biotransformation with 2,5-DKCMO-2-Fred yielded the "normal" lactone in 58% ee and the "abnormal" lactone in 20% ee at 59% reaction conversion. Purified 2,5-DKCMO was reported to give the "normal" lactone in 60% ee at 20% reaction conversion (28). Formation of the "abnormal" lactone was not reported. 3,6-DKCMO-Fred oxidized norcamphor exclusively to the "normal" lactone with excellent enantioselectivity (94% ee) at 26% reaction conversion. Similarly, purified 3,6-DKCMO was reported to give the "normal" lactone in >90% ee at 48 % conversion (28).

DISCUSSION

We have purified a camphor-inducible flavin reductase (Fred) from strain PpCam and this homodimeric protein of subunit M_r of 18-kDa was shown to be functionally competent in providing the required electrons to the respective monooxygenase component in the oxidation of a variety of substrates. A chromosomally-located Fred-encoding gene was cloned and enabled the first assembly of a *bona-fide* two-component system in a recombinant format for the

501 enantiomer-specific 2,5- and 3,6-DKCMOs. This DKCMO-Fred system represents the first
502 among the known FMN-dependent two-component monooxygenase systems (21) where a single
503 FMN reductase serves three separate monooxygenating components besides representing a single
504 step in the CAM degradation pathway (Fig. 1).

505 Contrary to a previously described oxidoreductase (14, 35, 36), Fred is not a flavoprotein.
506 The enzyme uses flavins (FMN in preference to FAD) only as substrates and thus it is not an
507 NADH oxidase and it is incapable of transfering electrons directly from NADH to molecular
508 oxygen. Fred also differs from the purified NADH oxidase (14, 35, 36) in that it is not a single
509 polypeptide of M_r 36-kDa but consists of two identical subunits of 18-kDa making it highly
510 unlikely that the homodimeric subunits would discriminate between FMN and FAD in regard to
511 their binding capacities: 1 mol/mol FMN, 2mol/mol FAD as described by Trudgill et al (35).
512 Other differences are in the isoelectric points (pI of 6.6 based on cellulose acetate electrophoresis
513 for NADH oxidase vs a theoretical pI of 4.97 for Fred), and the amino acid compositions (one
514 methionine, 4 half-cystines per mole of the former enzyme vs. the sequence-derived 4 cysteines
515 per subunit: 8 in total, and 4 methionines per subunit: 8 in total for Fred).

516 Characteristics of the strain PpCam Fred classify it a new member of the Class II
517 nonflavoprotein reductases, meaning that the flavin acts as a substrate for catalysis as opposed to
518 a tightly bound cofactor in Class I flavoprotein reductases (21, 52). The kinetic properties of
519 Fred toward FMN and NADH approximate those of FRD_H of *Beneckea harveyi* (52, 53). The
520 latter and a few others have been characterized to undergo a sequential mechanism of electron
521 transfer, i.e., the reduced flavin substrate is transferred to the monooxgenase component only
522 after its reduction by NADH (21). The conserved GDH motif in Fred implies that H136 may
523 play a critical role in NADH binding and reduction of the FMN cofactor, as it was first reported

524 for the NADH:flavin oxidoreductase (FRD_{Aa}) system of *Aminobacter animonvorans* (formerly,
525 NmoB or NtaB of *Chelatobacter heintzii*; 49). PpCam Fred also contains the conserved YGG
526 motif reported in the modeled structure of a flavin reductase of *Thermus thermophilus* HB8 that
527 uses FAD as substrate (50). This region was deemed important in substrate flavin binding by
528 deletion of the C-terminal 5 amino acids containing the YGG motif (50).

529 A second revelation of this study is the identification and localization of a duplicated set of
530 genes, $camE_{25\text{-}1}$ and $camE_{25\text{-}2}$ genes on the CAM plasmid that encode 2,5-DCKMO-1 and 2,5-
531 DKCMO-2. This unravels a 26-43 year old mystery first documented by Gunsalus and coworker
532 (54) and later by Trudgill (14) who although could not reproduce the presence of a "third"
533 component, referred to as E_2' in (54), provided electrophoretic evidence of two separable forms
534 of 2,5-DKCMO. The predicted charge difference between the two isozymes (pI 5.58 for
535 DCKMO-1 and 5.40 for DKCMO-2) would account for the electrophoretic separation in a native
536 gel (14). Clearly, the high sequence identity between $camE_{25\text{-}1}$ and $camE_{25\text{-}2}$ was the result of a
537 gene duplication event and sequence divergence in the case of $camE_{3,6}$. Identification of the
538 duplicated set of 2,5-DCKMO-encoding genes means that Kadow et al (25) had cloned the
539 $camE_{25\text{-}1}$ and all previously reported biotransformation results using whole cells of PpCam were
540 most likely the summation of the two DKCMO activities. Interestingly, the N-terminal amino
541 acid sequence experimentally determined for one DKCMO (15, 31) actually has a better match
542 to that of DKCMO-2 than DKCMO-1 (Supplemental material Fig. S3b).

543 With the reconstituted and "personalized" DKCMO-Fred plasmid systems we confirmed the
544 enantiomeric specificity of the 2,5-DCKMO and 3,6-DKCMO enzymes for the (+) and (–)
545 camphor as previously reported (13, 14). On the other hand, contradictory results were presented
546 by Kadow et al (25, 26) who relied on an unknown factor in *E. coli* to effect substrate oxidations.

547 Given the current spectrum of substrates, the oxidation effected by the two 2,5-DKCMO
548 isozymes so far appear indistinguishable. For synthetic purpose, most notable result is the
549 specificity toward the (*R*)-enantiomer of 2-phenylcyclohexanone (**12**) that rendered an *E* value of
550 >200 in both cases (Table 3). The action of 3,6-DKCMO is most different with regard to
551 oxidation of norcamphor (**18**) where it provided the "normal" lactone exclusively with excellent
552 enantioselectivity (94% ee) at 26% reaction conversion (Table 5).

553 Although CAM plasmid is widely known as one of the oldest known degradative plasmids
554 alongside SAL, NAH and OCT plasmids that are responsible for the degradation of salicylate,
555 naphthalene and octane, respectively (2, 55) its molecular size has been largely propagated in the
556 literature as 150-MDa or 236-250 kb (e.g. 25). Here, by the criteria of PFGE the CAM plasmid
557 was determined to have a size of ~530-kb, besides being linear. A covalently closed circular
558 plasmid would exhibit a constant migration pattern in the PFGE that is independent of the pulse
559 conditions (see SM2 note in supplemental material).

560 As per gene elucidation of the CAM degradation pathway, eight catabolic genes responsible
561 for four biochemical steps besides the regulatory *camR*, are now presently known and
562 characterized (8, 10-12, 24, 25, 29, this study). By sequence homology, additional ORFs that
563 could account for the remaining steps of the degradation pathway are presented in Fig. S3 of
564 supplemental material. It is interesting to note that besides the well characterized TetR-type
565 *camR* repressor that regulates the P-450cam hydroxylase operon (56), four potential
566 transcriptional repressors (orf5[CamS], orf11[CamU] and orf20[CamV] of TetR-type; and
567 orf7[CamT] of LysR-type) with limited sequence identity to each other with the exception of
568 Orf20[CamV] and CamR (54% identity), decorate the sequenced *cam* locus (Fig. 2). Clearly,
569 regulation of the entire *cam* pathway is complicated which is beyond the scope of this study.

570 Suffice it to say that the *camE*$_{25\text{-}1}$ and *cam*G and those of *camE*$_{25\text{-}2}$ and *camE*$_{36}$ are predicted to be
571 divergently transcribed as per position on opposite DNA strand. Interestingly, this supports an
572 earlier observation that the MO1 (mixtures of 2,5- and 3,6-DKCMO) and MO2 (OTEMO)
573 activities are not "coordinately controlled." (27).

574 In conclusion, the availability of the recombinant format of the three DKCMO-Fred systems
575 opens up new opportunities in organic synthesis besides the production of camphor lactones.
576 Access to exquisite sulfoxide synthons by "separated" DKCMO is a potentially grand
577 opportunity, made possible previously by using "washed whole cells" of strain PpCam (30).
578 With regard to mechanistic study, the new DKCMO-Fred systems provide an unique model for
579 structure-function analyses of a special enantiocomplementary kind where a single flavin
580 reductase serves three separate monooxygenating components. Are there differences in the
581 mechanism of flavin transfer from the reductase to the DKCMO enantiomeric pair is just one
582 more question in the complexity of flavoenzymology (21, 57).

583

584 **ACKNOWLEDGMENTS**

585 Funding by NRC through the National Bioproducts Program is gratefully acknowledged. This
586 work was financially supported in part by the Kansai University Expenditure for cultivating
587 young researchers (2012) provided to H. Iwaki. This paper is dedicated to the memory of late
588 Irwin C. (Gunny) Gunsalus (1912-2008), whose middle initial although stands for Clyde, should
589 be synonymous with camphor or cytochrome P450$_{cam}$.

590

591 **REFERENCES**

1. **Bradshaw WH, Conrad HE, Corey EJ, Gunsalus IC, Lednicer D.** 1959. Microbiological degradation of (+)-camphor. J. Am. Chem. Soc. **81:**5507.
2. **Rheinwald JG, Chakrabarty AM, Gunsalus IC.** 1973. A transmissible plasmid controlling camphor oxidation in *Pseudomonas putida*. Proc. Natl. Acad. Sci. USA. **70:**885-889.
3. **Sokatch JR.** (1986) The Bacteria. Vol. 10. *The biology of Pseudomonas*. Acad. Press, Inc. Harcourt Brace, Jovanovich, Publishers.
4. **Conrad HE, Dubus R, Gunsalus IC.** 1961. An enzyme system for cyclic ketone lactonization. Biochem. Biophys. Res. Commun. **6:**293-297.
5. **Conrad HE, Dubus R, Namtvedt MJ, Gunsalus IC.** 1965. Mixed function oxidation. II. Separation and properties of the enzyme catalysing camphor lactonization. J. Biol. Chem. **240:**495-503.
6. **Conrad HE, Leib K, Gunsalus IC.** 1965**.** Mixed function oxidation. III. An electron transport complex in camphor ketolactonization. J. Biol. Chem. **240:**4029-4037.
7. **Ougham HJ, Taylor DG, Trudgill PW.** 1983. Camphor revisited: Involvement of a unique monooxygenase in metabolism of 2-oxo-Δ^3-4,5,5-trimethylcyclopentenylacetic acid by *Pseudomonas putida*. J. Bacteriol. **153:**140-152.
8. **Unger P, Sligar SG, Gunsalus IC.** 1986. *Pseudomonas* cytochromes P-450, p. 557-589. *In* J.R. Sokatch (ed.), The Bacteria, Vol 10, Academic Press, New York.
9. **Trudgill PW.** 1986. Terpenoid metabolism by *Pseudomonas.* p483-525. *In* J.R. Sokatch and L.N. Ornston (ed.), The bacteria: a treatise on structure and function. The biology of *Pseudomonas*. Acad. Press. Inc. Orlando, Fla.

10. **Koga H, Aramakim H, Yamaguchi E, Takeuchi K, Horiuchi T, Gunsalus IC.** 1986. *camR*, a negative regulator locus of the cytochrome P-450_{cam} hydroxylase operon. J. Bacteriol. **166:**1089-1095.
11. **Koga H. Yamaguchi E, Matsunaga K, Aramaki H, Horiuchi T.** 1989. Cloning and nucleotide sequence of NADH-putidaredoxin reductase gene (*camA*) and putidaredoxin gene (*camB*) involved in cytochrome P-450_{cam} hydroxylase of *Pseudomonas putida*. J. Biochem. **106:**831-836.
12. **Fujita M, Aramaki H, Horiuchi T, Amemura A.** 1993. Transcription of the *cam* operon and *camR* genes in *Pseudomonas putida* PpG1. J. Bacteriol. **175:**6953-6958.
13. **Jones KH, Smith RT, Trudgill PW.** 1993. Diketocamphane enantiomer-specific "Baeyer–Villiger" monooxygenases from camphor-grown *Pseudomonas putida* ATCC 17453. Gen. Microbiol. **139:**797-805.
14. **Taylor DG, Trudgill PW.** 1986. Camphor revisited: Studies of 2,5-diketocampane 1,2-monooxygenase from *Pseudomonas putida* ATCC 17453. J. Bacteriol. **165:**489-497.
15. **Willetts A.** 1997. Structural studies and synthetic applications of Baeyer-Villiger monooxygenases. Trends Biotech. **15:**55-62.
16. **Alphand V, Wohlgemuth R.** 2010. Applications of Baeyer-Villiger monooxygenases in organic synthesis. Curr. Org. Chem. **14:**1928-1965.
17. **De Gonzolo G, Mihovilovic MD, Fraaije MW.** 2010. Recent developments in the application of Baeyer-Villiger monooxygenases as biocatalysts. ChembioChem **11:**2208-2231.
18. **Leisch H, Morley K, Lau PCK.** 2011. Baeyer-Villiger monooxygenases: More than just green chemistry. Chem. Rev. **111:**4165-4222.

19. **Zhang ZG, Parra LP, Reetz MT.** 2012. Protein engineering of stereoselective Baeyer-Villiger monooxygenases. Chemistry. **18:**10160-10172.
20. **Bornscheuer UT, Huisman GW, Kazlauskas RJ, Lutz S, Moore JC, Robins K.** 2012. Engineering the third wave of biocatalysis. Nature. **485:**185-194.
21. **Ellis HR.** 2010. The FMN-dependent two-component monooxygenase systems. Arch. Biochem. Biophys. **497:**1-12.
22. **McGhie EJ, Littlechild J.** 1996. The purification and crystallisation of 2,5-diketocamphane 1,2 monooxygnenase and 3,6-ketocamphane 1,6 monooxygenase from *Pseudomonas putida* NCIMB 10007. Biochem. Soc. Trans. 29S.
23. **McGhie EJ, Isupov MN, Schroder E, Littlechild J.** 1998. Crystallization and preliminary X-ray diffraction studies of the oxygenating subunit of 3,6-ketocamphane monooxygenase from *Pseudomonas putida*. Acta Cryst. **D54:**1035-1038.
24. **Isupov MN, Lebedev AA.** 2008. NCS-constrained exhaustive search using oligomeric models. Acta Cryst. **D64:**90-98.
25. **Kadow M, Saß S**, **Schmidt M, Bornscheuer UT. 2011.** Recombinant expression and purification of the 2,5-diketocamphane 1,2-monooxygenase from the camphor metabolizing *Pseudomonas putida* strain NCIMB 10007. AMB Express **1:**13.
26. **Kadow M, Loschinski K, Saß S**, **Schmidt M, Bornscheuer UT.** 2012. Completing the series of BVMOs involved in camphor metabolism of *Pseudomonas putida* NCIMB 10007 by identification of the two missing genes, their functional expression in *E. coli*, and biochemical characterization. Appl. Microbiol. Biotechnol. **96:**419-429.

27. **Grogan G, Roberts S, Wan P, Willetts A.** 1993. Camphor-grown *Pseudomonas putida*, a multifunctional biocatalyst for undertaking Baeyer-Villiger monooxygenase-dependent biotransformations. Biotech. Lett. **15:**913-918.

28. **Gagnon R, Grogan G, Levitt MS, Roberts SM, Wan PWH, Willetts AJ.** 1994. Biological Baeyer-Villiger oxidation of some monocyclic and bicyclic ketones using monooxygenases from *Acinetobacter calcoaceticus* NCIMB 9871 and *Pseudomonas putida* NCIMB 10007. J. Chem. Soc. Perkin Trans. 2537-2543.

29. **Leisch H, Shi R, Grosse S, Morley K, Bergeron H, Cygler M, Iwaki H, Hasegawa Y, Lau PCK.** 2012. Cloning, Baeyer-Villiger biooxidations, and structures of the camphor pathway 2-oxo-3-4,5,5-trimethylcyclopentenylacetyl-Coenzyme A monooxygenase of *Pseudomonas putida* ATCC 17453. Appl. Environ. Microbiol. **78:**2200-2212.

30. **Beecher J, Richardson P, Willetts A.** 1994. Baeyer-Villiger monooxygenase-dependent biotransformations: Stereospecific heteroatom oxidations by camphor-grown *Pseudomonas putida* to produce chiral sulfoxides. Biotechnol. Letts **16:**909-912.

31. **Beecher J, Grogan G, Roberts S, Willetts A.** 1996. Enantioselective oxidations by the diketocamphane monooxygenase isozymes from *Pseudomonas putida*. Biotechnol. Letts **18:**571-576.

32. **Beecher J, Willetts A.** 1998. Biotransformation of organic sulfides. Predictive active site models for sulfoxidation catalysed by 2,5-diketocamphane 1,2-monooxygenase and 3,6-diketocamphane 1,6-monooxygenase, enantiocomplementary enzymes from *Pseudomonas putida* NCIMB 10007. Tetrahedron Asymm. **9:**1899-1916.

33. **Gagnon R, Grogan G, Roberts SM, Villa R, Willetts AJ.** 1995. Enzymatic Baeyer-Villiger oxidations of some bicyclo[2.2.1]heptan-2-ones using monooxygenases from

Pseudomonas putida NCIMB 10007: enantioselective preparation of a precursor of azadirachtin. J. Chem. Soc. Perkin Trans. 1505-1511.

34. **Conrad HE, Hedegaard J, Gunsalus IC, Corey EJ, Uda H.** 1965. Lactone intermediates in the microbial oxidation of (+)-camphor. Tetrahedron Lett. **6:**561-565.
35. **Trudgill, PW, DuBus R, Gunsalus IC.** 1966a. Mixed function oxidation: V. Flavin interaction with a reduced diphosphopyridine nucleotide dehydrogenase, one of the enzymes participating in camphor lactonization. J. Biol. Chem. **241:**1194-1205.
36. **Trudgill PW, DuBus R, Gunsalus IC.** 1966b. Mixed function oxidation: VI. Purification of a tightly coupled electron transport complex in camphor lactonization. J. Biol. Chem. 241:4288-4290.
37. **Pedraza RO, Ricci JCD.** 2002. In-well cell lysis technique reveals two new megaplasmids of 103.0 and 212.6 MDa in the multiple plasmid-containing strain V517 of *Escherichia coli*. Lett. Appl. Microbiol. **34**:130–133.
38. **Barton BM, Harding GP, Zuccarelli AJ.** 1995. A general method for detecting and sizing large plasmids. Anal. Biochem. 226**:**235-240.
39. **Romine MF, Stillwell LC, Wong KK, Thurstone SJ, Sisk EC, Sensen C, Gassterland T, Fredrickson JK, Saffer JD.** 1999. Complete sequence of a 184-kilobase catabolic plasmid from *Sphingomonas aromaticivorans* F199. J. Bacteriol. **181:**1585-1602.
40. **Bergeron H, Labbé D, Turmel C, Lau PCK.** (1998) Cloning, sequence and expression of a linear plasmid-based and a chromosomally homolog of chloroacetaldehyde dehydrogenase-encoding genes in *Xanthobacter autotrophicus* GJ10. Gene **207:**9-18.
41. **Sambrook J, Fritsch EF, Maniatis T.** 1989. Molecular cloning: a laboratory manual, 2nd ed. Cold Spring Harbor Laboratory Press, Cold Spring Harbor, N.Y.

42. **Smith SP, Barber KR, Dunn SD, Shaw GS.** 1996. Structural influence of cation binding to recombinant human brain S100b: evidence for calcium-induced exposure of a hydrophobic surface. Biochemistry **35:**8805-8814.

43. **Iwaki H, Hasegawa Y, Wang S, Kayser MM, Lau PCK.** 2002. Cloning and characterization of a gene cluster involved in cyclopentanol metabolism in *Comamonas* sp. strain NCIMB 9872 and biotransformations effected by *Escherichia coli*-expressed cyclopentanone 1,2-monooxygenase. Appl. Environ. Microbiol. **68:**5671-5684.

44. **Iwaki H, Wang S, Grosse S, Bergeron H, Nagahashi A, Lertvorachon J, Yang J, Konishi Y, Hasegawa Y, Lau PCK.** 2006. Pseudomonad cyclopentadecanone monooxygenase displaying an uncommon spectrum of Baeyer-Villiger oxidations of cyclic ketones. Appl. Environ. Microbiol. **72:**2707-2720.

45. **Edman P, Henschen A.** 1975. Sequence determination, p. 232-279. In S.B. Needleman (ed.), Protein Sequence Determination, Springer, Berlin.

46. **Mahoney WC, Hermodson MA.** 1979. High-yield cleavage of tryptophanyl peptide bonds by o-iodosobenzoic acid. Biochemistry. **18:**3810-3814.

47. **Skopp RN, Lane LC.** 1988. Fingerprinting of proteins cleaved in solution by cyanogen bromide. Appl. Theor. Electroph. **1:**61–64.

48. **Piszkiewicz D, Landon M, Smith EL.** 1970. Anomalous cleavage of aspartyl-proline peptide bonds during amino acid sequence determinations. Biochem. Biophys. Res. Commun. **40:**1173–1178.

49. **Russell TR, Tu SC.** 2004. *Aminobacter aminovorans* NADH:flavin oxidoreductase His 140: A highly conserved residue critical for NADH binding and utilization. Biochem. **43:**12887-12893.

50. **Imagawa T, Tsurumura T, Sugimoto Y, Aki K, Ishidoh K, Kuramitsuu S, Tsuge H.** 2011. Structural basis of free reduced flavin generation by flavin reductase from *Thermus thermophilus* HB8. J. Biol.Chem. **286:**44078-44085.

51. **Zhang Y, Edwards TE, Begley DW, Abramov A, Thompkins KB, Ferrell M, Guo WJ, Phan I, Olsen C, Napuli A, Sankaran B, Stacey R, van Voorhis WC, Stewart LJ, Myler PJ.** 2011. Structure of nitrilotriacetate monooxygenase component B from *Mycobacterium thermoresistibile*. Acta Crys. **F67:**1100-1105.

52. **Tu SC.** 2001. Reduced flavin: Donor and acceptor enzymes and mechanisms of channeling. Antioxidants and Redox Signaling. 3:881-897.

53. **Jablonski E, DeLuca M.** 1978. Studies of the control of luminescence in *Beneckea harveyi*: Properties of the NADH and NADPH:FMN oxidoreductases Biochemistry, **17:**672-678.

54. **Yu CA, Gunsalus IC.** 1969. Monooxygenases*:* VII. Camphor ketolactonase I and the role of three protein components**.** J. Biol. Chem. **244:**6149-6152.

55. **Chakrabarty AM.** 1976. Plasmids in *Pseudomonas*. Ann. Rev. Genet. **10:**7-30.

56. **Aramaki H, Sagara Y, Hosoi M, Horiuchi T.** 1993. Evidence for autoregulation of *camR*, which encodes a repressor for the cytochrome P-450cam hydroxylase operon on the *Pseudomonas putida* CAM plasmid. J. Bacteriol. **175:**7828-7833.

57. **Chaiyen P, Fraaije MW, Mattevi A.** 2012. The enigmatic reaction of flavins with oxygen. Trends Biotech. **39:**373-380.

List of Tables

Figure legends

FIG 1. Metabolism of camphor isomers to acetyl-CoA and isobutyryl-CoA in *Pseudomonas putida* ATCC 17453. Modified from Leisch et al. (29) with cumulative data from references 7, 9, 11. Nomenclature of *camE* for the oxygenating components of diketocamphane (DKC) monooxygenase isozymes (DKCMO) was adapted from Koga et al. (10). Fred is a short-chain flavin reductase (this study). The lactones of DKC monooxygenations are presumed to undergo spontaneous hydrolysis to form compound **5** (9). *camF1/F2* are putative genes for 2-oxo-Δ^3-4,5,5-trimethylcyclopentenylacetyl-CoA synthetase (Fig. S1 in supplemental material) that produce the carbonyl-CoA (COSCoA) derivative of **5**, a substrate for OTEMO (type 1 BVMO; 29). HSCoA, acetyl-CoA. Additional steps of the degradation pathway are in discussed in Fig. S1 of supplemental material.

FIG 2. Localization of additional genes and predicted open reading frames (ORFs) flanking the established initial genes of the camphor *camDCAB* operon and its repressor, *camR* on a ~40.5-kb sequenced region of the CAM plasmid of *P. putida* ATCC 17453. The predicted ORFs or genes

773 are numbered from 1-27 except for the established *camRDCAB* that are shaded in black. The
774 orientation of the arrows indicates the direction of gene transcription. The candidate genes of
775 this study ($camE_{25\text{-}1;\ 25\text{-}2}$ and $camD_{36}$) representing the three diketocamphane monooxygenase
776 (DKCMO) isozymes are highlighted in grey. The previously established OTEMO-encoding gene
777 (29) has been designated *camG* following the respective catabolic steps (see Fig. 1). *camS, T, U*
778 *and V* are potential transcriptional regulators, *camV* is a close homolog of *camR*. Rationale for
779 the predicted ORFs and the various subclones and the probe regions to cover the sequenced
780 CAM plasmid locus are elaborated in the SM1/Table S1/S2/Fig. S1of supplemental material. The
781 black solid line represents the previously sequenced region with the indicated GenBank
782 accession numbers.
783
784 FIG 3. Establishing linearity of CAM plasmid of *P. putida* ATCC17453 by pulsed field gel
785 electrophoresis. Lane 1. Lambda ladder PFG marker DNA with some indicated size in kb
786 alongside; Lanes 3 and 5 are S1-nuclease treated *S. aromaticivorans* and CAM plasmid DNA
787 preparations, respectively. Lanes 2 and 4 are S1 nuclease–non treated samples of *S.*
788 *aromaticivorans* F199 and CAM plasmid DNAs, respectively. A, B and C indicate the estimated
789 plasmid sizes of CAM plasmid (533-kb) of strain PpCam, pNL2 (485-kb) and pNL1 (185-kb) of
790 strain F199, respectively.
791
792 FIG 4. Purification scheme and SDS-PAGE (12% PA) of 18–kDa FMN-reductase (Fred) from *P.*
793 *putida* ATCC 17453. Units of enzyme activity are defined by the amount of protein which
794 oxidizes one μmole of NADH ($\varepsilon = 6.22$ L mmol^{-1} cm^{-1}) per min using FMN as substrate. Protein

795 standards (ovalbumin, carbonic anhydrase, lysozyme) of decreasing sizes are indicated
796 alongside. The purified Fred as shown is after the final size exclusion step.
797
798
799 FIG 5. Protein sequence alignment of PpCam flavin reductase (Fred) with short-chain flavin
800 reductases of known structures with top scores from the PDB entries. 3NFW, nitrilotriacetate
801 monooxygenase component B of *Mycobacterium thermoresistibile*, 40.5% identity; 3PFT, flavin
802 reductase (DszD) of *M. goodii*, 29.8% identity; 1RZ0, flavin reductase (PheA2) of phenol 2-
803 hydroxylase of *Bacillus thermoglucosidasius* A7, 28.8% identity; and 2ECR, flavin reductase
804 (HpaC) of hydroxyphenylacetate 3-monooxygenase of *Thermus thermophilus* HP8, 25.1%
805 identity. The secondary structural elements of 3NFW are indicated and labelled above the
806 aligned sequences. The predicted secondary structural elements of Fred using the Psipred
807 program (http://bioinf.cs.ucl.ac.uk/psipred/) are shown below. The consensus amino acids of the
808 aligned sequences including ten entirely conserved residues are highlighted.
809
810 FIG 6. Potentiation of 2,5-DKCMO activity by the addition of FMN-reductase (Fred).
811 Remaining (+)-camphor (•) was monitored by HPLC with a constant amount of 2,5-DKCMO-2
812 while increasing the Fred concentration. Reaction incubation time was 30 min. The resulting
813 increment in DKCMO activity is as indicated (▾).
814
815
816

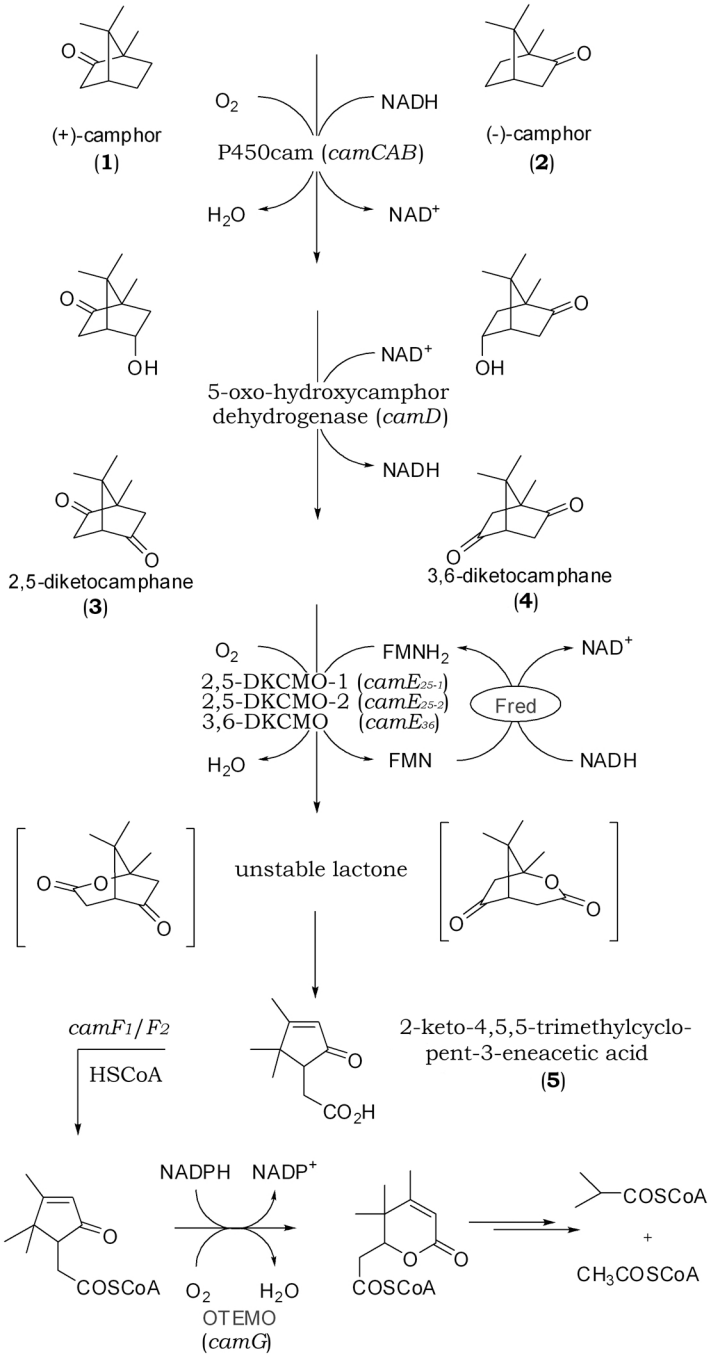
(+)-camphor
(1)
O2
NADH
P450cam (camCAB)
H2O
NAD+
(-)-camphor
(2)
OH
NAD+
5-oxo-hydroxycamphor
dehydrogenase (camD)
NADH
OH
2,5-diketocamphane
(3)
3,6-diketocamphane
(4)
O2
FMNH2
2,5-DKCMO-1 (camE25-1)
2,5-DKCMO-2 (camE25-2)
3,6-DKCMO (camE36)
H2O
FMN
Fred
NAD+
NADH
unstable lactone
camF1/F2
HSCoA
CO2H
2-keto-4,5,5-trimethylcyclo-
pent-3-eneacetic acid
(5)
NADPH
NADP+
O2
H2O
OTEMO
(camG)
COSCoA
COSCoA
COSCoA
+
CH3COSCoA

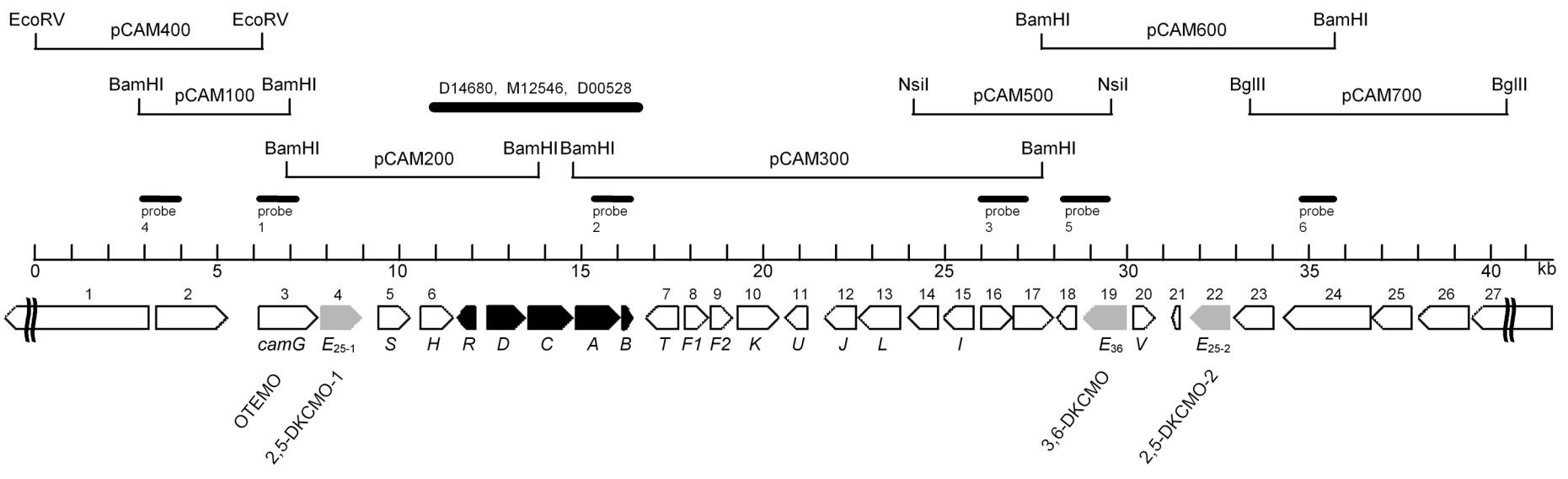
EcoRV
pCAM400
EcoRV
BamHI
pCAM600
BamHI
BamHI
pCAM100
BamHI
D14680, M12546, D00528
NsiI
pCAM500
NsiI
BglII
pCAM700
BglII
BamHI
pCAM200
BamHI
BamHI
pCAM300
BamHI
probe 4
probe 1
probe 2
probe 3
probe 5
probe 6
0
5
10
15
20
25
30
35
40
kb
camG
E25-1
S
H
R
D
C
A
B
T
F1
F2
K
U
J
L
I
E36
V
E25-2
OTEMO
2,5-DKCMO-1
3,6-DKCMO
2,5-DKCMO-2

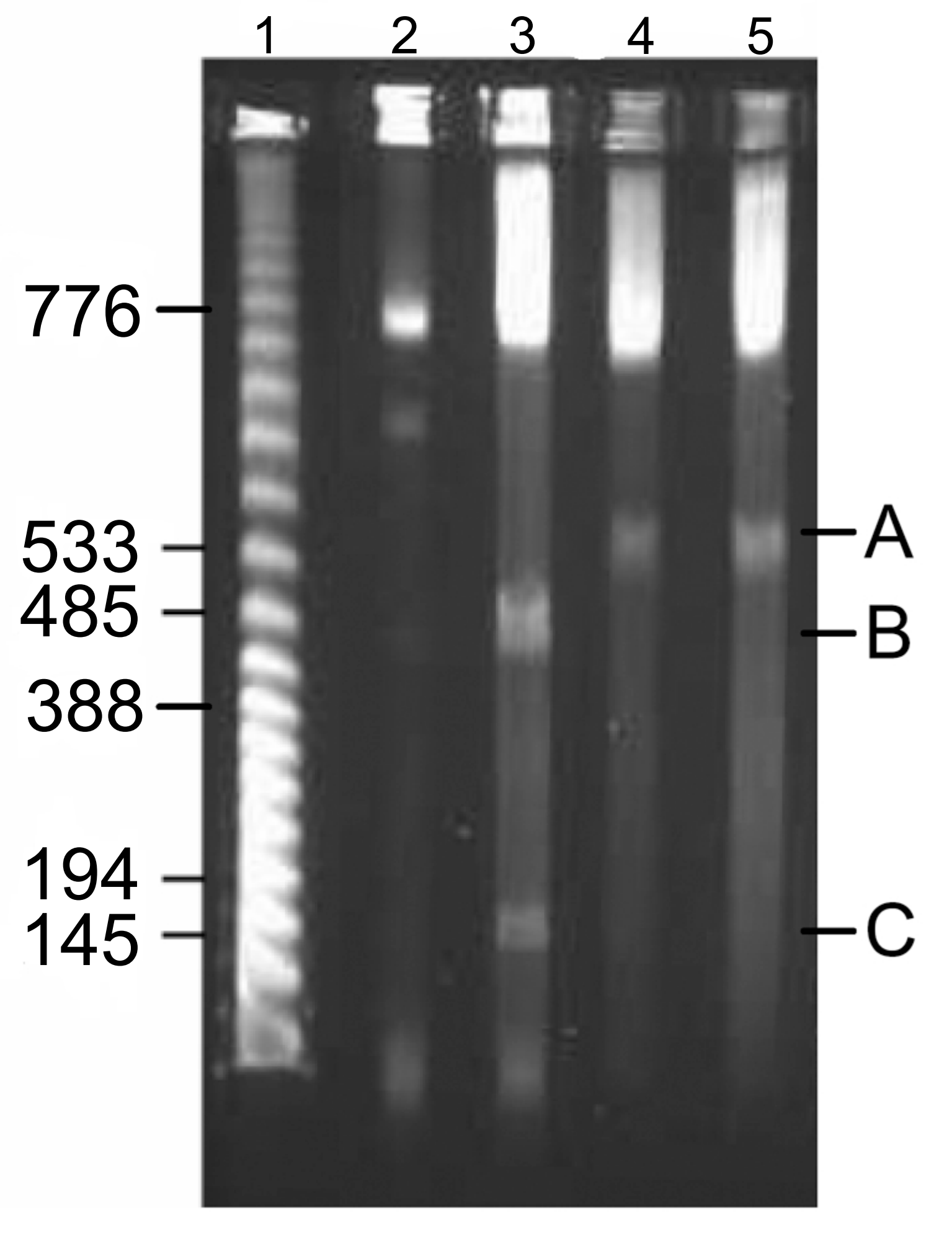
1
2
3
4
5
776
533
485
388
194
145
A
B
C

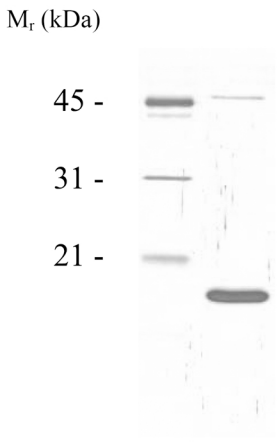

Purification step	Tot. Prot. (mg)	Tot. Act. (U)	Spec. Act. (U/mg)	Yield/Purif. (% / fold)
Crude extract	4,200	10,080	2.4	100 / 1
DEAE-Seph.	160	4,692	29.2	47 / 12
Ni-NTA	18	3,248	176.9	32 / 74
Superdex 200	3	1,791	628.4	18 / 262

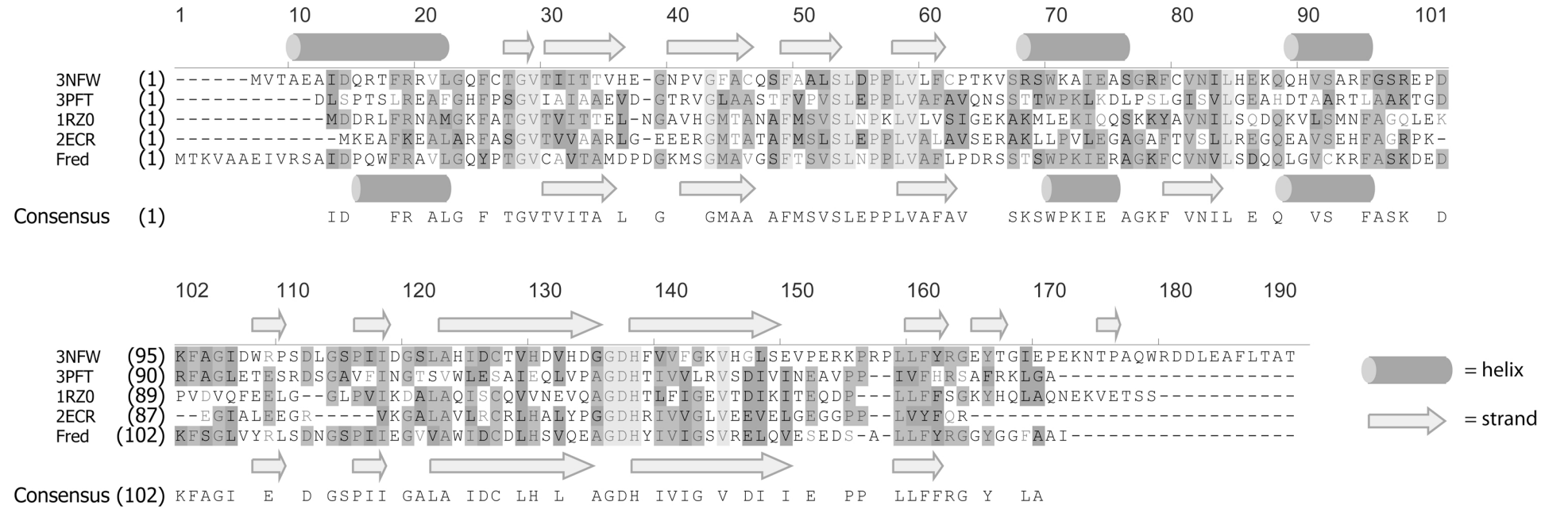
1 10 20 30 40 50 60 70 80 90 101
3NFW (1) ------MVTAEAIDQRTFRRVLGQFCTGVTIITTVHE-GNPVGFACQSFAALSLDPPLVLFCPTKVSRSWKAIEASGRFCVNILHEKQQHVSARFGSREPD
3PFT (1) ----------DLSPTSLREAFGHFPSGVIAIAAEVD-GTRVGLAASTFVPVSLEPPLVAFAVQNSSTTWPKLKDLPSLGISVLGEAHDTAARTLAAKTGD
1RZ0 (1) ----------MDDRLFRNAMGKFATGVTVITTEL-NGAVHGMTANAFMSVSLNPKLVLVSIGEKAKMLEKIQQSKKYAVNILSQDQKVLSMNFAGQLEK
2ECR (1) ----------MKEAFKEALARFASGVTVVAARLG-EEERGMTATAFMSLSLEPPLVALAVSERAKLLPVLEGAGAFTVSLLREGQEAVSEHFAGRPK-
Fred (1) MTKVAAEIVRSAIDPQWFRAVLGQYPTGVCAVTAMDPDGKMSGMAVGSFTSVSLNPPLVAFLPDRSSTSWPKIERAGKFCVNVLSDQQLGVCKRFASKDED
Consensus (1) ID FR ALG F TGVTVITA L G GMAA AFMSVSLEPPLVAFAV SKSWPKIE AGKF VNIL E Q VS FASK D
102 110 120 130 140 150 160 170 180 190
3NFW (95) KFAGIDWRPSDLGSPIIDGSLAHIDCTVHDVHDGGDHFVVFGKVHGLSEVPERKPRPLLFYRGEYTGIEPEKNTPAQWRDDLEAFLTAT
3PFT (90) RFAGLETESRDSGAVFINGTSVWLESAIEQLVPAGDHTIVVLRVSDIVINEAVPP--IVFHRSAFRKLGA----------
1RZ0 (89) PVDVQFEELG--GLPVIKDALAQISCQVVNEVQAGDHTLFIGEVTDIKITEQDP---LLFFSGKYHQLAQNEKVETSS----------
2ECR (87) --EGIALEEGR-----VKGALAVLRCRLHALYPGGDHRIVVGLVEEVELGEGGPP--LVYFQR----------
Fred (102) KFSGLVYRLSDNGSPIIEGVVAWIDCDLHSVQEAGDHYIVIGSVRELQVESEDS-A-LLFYRGGYGGFAAI----------
Consensus (102) KFAGI E D GSPII GALA IDC LH L AGDH IVIG V DI I E PP LLFFRG Y LA
= helix
= strand

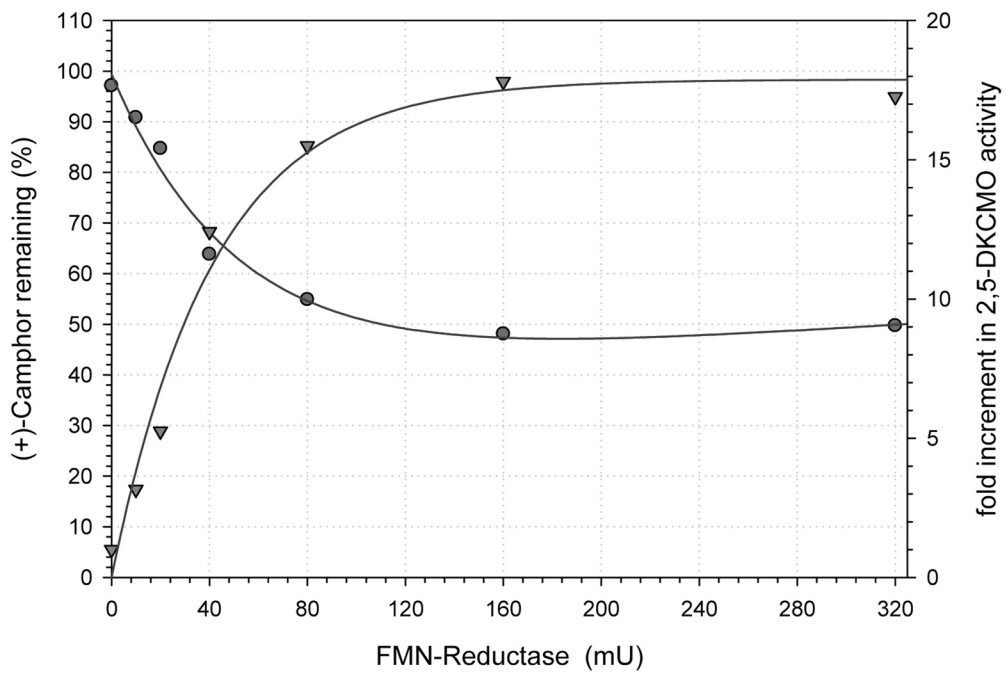
(+)-Camphor remaining (%)
fold increment in 2,5-DKCMO activity
FMN-Reductase (mU)
0
10
20
30
40
50
60
70
80
90
100
110
0
5
10
15
20
0
40
80
120
160
200
240
280
320

Table 1. Oxidation of terpenones

Substrate	2,5-DKCMO-1 +Fred	2,5-DKCMO-2 +Fred	3,6-DKCMO + Fred	Product
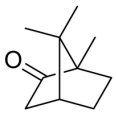 **1**	100%	100%	0%	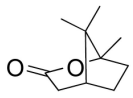 **1a**
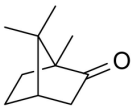 **2**	0%	0%	100%	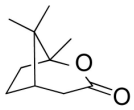 **2a**
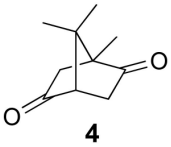 **4**	0%	0%	100%	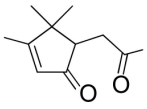 **5**
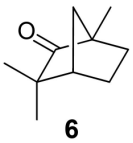 **6**		No conversion		
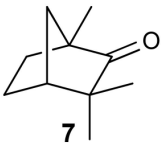 **7**		No conversion		
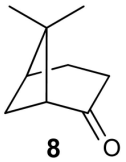 **8**		No conversion		

Table 2. Kinetic resolution of racemic ketones

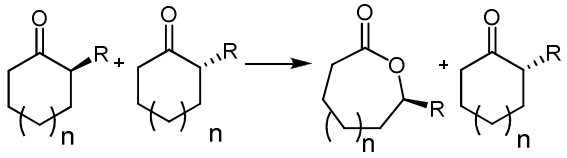

9 - 14 **9 - 14a** **9 - 14**

Substrate			2,5-DKCMO-1 +Fred		2,5-DKCMO-2 +Fred		3,6-DKCMO +Fred	
#	**n**	**R**	**Conv.[a] %**	***E*[b]**	**Conv. %**	***E***	**Conv. %**	***E***
9	1	Me	8	3.2 (*S*)	4	3.1 (*S*)	2	3.2 (*S*)
10	1	Et	11	43 (*S*)	6	22 (*S*)	0	n.a.[c]
11	1	Pr	18	19 (*S*)	13	8.5 (*S*)	trace	n.a.
12	1	Ph	23	>200 (*R*)	4	>200 (*R*)	2	1
13	0	Me	0	n.a.	0	n.a.	0	n.a.
14	0	He	6	12 (*S*)	3	5 (*S*)	0	n.a.

[a] determined by chiral GC based on area percentage; [b] Values were calculated according to a program available at ftp://biocatalysis.uni-graz.at/pub/enantio/ ; [c] not available.

Table 3. Desymmetrization of prochiral ketones.

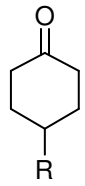

15 R = methyl
16 R = ethyl
17 R = *n*-pentyl
18 R = *tert*-butyl

Subst.	2,5-DKCMO-1 + Fred		2,5-DKCMO-2 + Fred		3,6-DKCMO + Fred	
	Conv.[a] %	*ee*[b] %	Conv. %	*ee* %	Conv. %	*ee* %
15	8	27 (*R*)	5	55 (*R*)	Traces	n.a.[c]
16	29	71 (*R*)	10	89 (*R*)	3	87 (*S*)
17	2	26 (*R*)	traces	n.a.	0	n. a.
18	5	61 (*S*)	traces	n.a.	0	n.a.

[a] determined by chiral GC based on area percentage; [b] determined by chiral GC; [c] not available.

Table 4. Regiodivergent oxidations of bicyclic ketones.

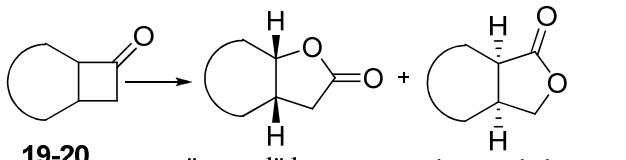

19-20 "normal" lactone **19-20a** "abnormal" lactone **19-20b**

Substrate	Biocat.	Conv. %	"normal" lactone	"abnormal" lactone
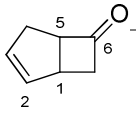 **19**	2,5-DKCMO-1 + Fred	100	ratio 1.3 : 1 77% ee (1*R*,5S)	99% ee (1*S*,5*R*)
	2,5-DKCMO-2 + Fred	100	ratio 1.1 : 1 87% ee (1*R*,5S)	97% ee (1*S*,5*R*)
	3,6-DKCMO + Fred	53	ratio 1 : 1.5 57% ee (1*R*,5S)	93% ee (1*S*,5*R*)
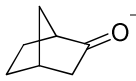 **20**	2,5-DKCMO-1 + Fred	64[a]	ratio 2.4 : 1 40% ee (1*R*,5S)	57% ee (1*R*,5S)
	2,5-DKCMO-2 + Fred	59[b]	ratio 1.8 : 1 58% ee (1*R*,5S)	20% ee (1*R*,5S)
	3,6-DKCMO + Fred	26[c]	only normal lactone 94% ee (1*R*,5S)	0

[a.] Starting material 98% ee; [b.] Starting material 89% ee; [c.] Starting material 45% ee